STUDIA INFORMATICA 2004
Volume 25 Number 3 (59)

Katarzyna STĄPOR, Adam ŚWITOŃSKI
Politechnika Śląska, Instytut Informatyki

BLOOD VESSELS SEGMENTATION FROM FUNDUS EYE IMAGES USING MATHEMATICAL MORPHOLOGY

Summary. In this paper the new method for automatic segmentation of blood vessels from fundus eye images is proposed. The proposed method is composed of the following steps; 1) contrast enhancement, 2) denoising, 3) vessels detection, 4) classification.

Keywords: mathematical morphology, top-hat transformation, fundus eye image.

SEGMENTACJA NACZYŃ KRWIONOŚNYCH NA CYFROWYCH OBRAZACH DNA OKA ZA POMOCĄ METOD MORFOLOGII MATEMATYCZNEJ

Streszczenie. W artykule przedstawiono nową metodę automatycznej segmentacji naczyń krwionośnych na cyfrowych obrazach dna oka. Zaproponowana metoda składa się z następujących kroków: 1) polepszanie kontrastu, 2) odszumianie, 3) detekcja naczyń, 4) klasyfikacja.

Słowa kluczowe: morfologia matematyczna, transformacja czubek-kapelusza, cyfrowy obraz dna oka.

1. Introduction

In ophthalmology, the automatic detection of blood vessels may be of considerable interest for computer assisted diagnosis. Finding the main components in fundus images like for example blood vessels helps in characterizing detected lesions (like for example microaneurysms, exudates) and in identifying false positives. Furthermore, vessel detection is interesting for the computation of parameters related to the blood flow. The vessels can be considered as landmarks of the fundus images, that may be used afterwards for image

registration of images taken at different times or using different methods. To perform a robust feature based registration, it is indispensable to rely on a robust and fast algorithm for vessel detection. Vessels are the only features that are common to every image of the retina. Fig.1 shows a typical fundus eye image taken from a fundus-camera.

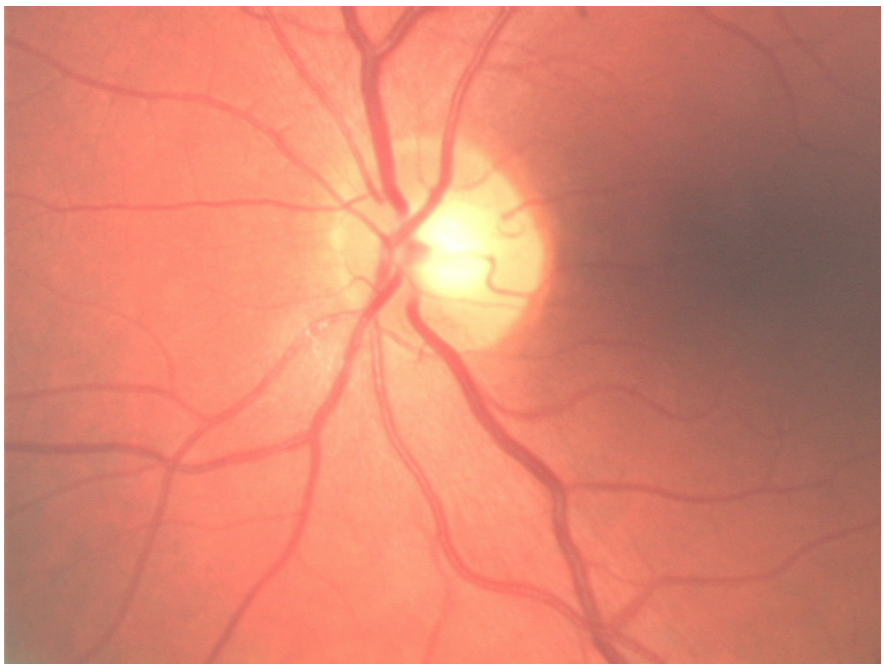

Fig. 1. The exampled fundus eye image
Rys. 1. Przykładowy obraz dna oka

Vessels appear darker than the background, their width is always smaller than a certain value, they are piecewise linear and they are connected in a tree like way. However, these properties hold only approximately: due to a presence of noise, the vessels are disconnected, and not each pixel on a vessel appears darker than the background. The vessel borders appear often unsharp.

Much has been written about the detection of vessels in medical images. Particularly for retinal images, matched filters [1], neural networks [5], a grouping algorithm of edgels [4] and a combination of linear and morphological methods [8] have been proposed.

In this paper we present the new, fast and robust algorithm for automatic vessel detection from color fundus eye images. The proposed algorithm is based on methods from mathematical morphology [6] and is composed of the following stages: 1) contrast enhancement, 2) denoising, 3) vessel detection, 4) classification.

2. Some gray-level morphological operators

In this section we briefly define the basic morphological operators used in this paper (for a comprehensive presentation see [6]). Let D_f and D_B be subsets of Z^2 and $T=\{t_{min}, \ldots, t_{max}\}$ be an ordered set of gray levels. A *gray-level image f* can be defined as a function:

$$f : D_f \subset Z^2 \to T \tag{1}$$

Furthermore, we define another image known as a *structuring element B*:

$$B : D_B \subset Z^2 \to T \tag{2}$$

We will restrict to flat, symmetric structuring elements B [6] and assume that point $(0,0) \in D_B$. We can now write the four basic morphological operators: *erosion*, *dilation*, *opening* and *closing* as:

(3)

(4)

Top-hat opening transformation is the difference between image *f* and opening of *f*:

$$TH_o^B(f)(x,y) = f(x,y) - O^B(f)(x,y) \tag{5}$$

Top-hat closing transformation is the difference between the closing transformation of *f* and the image *f*:

$$TH_c^B(f)(x,y) = C^B(f)(x,y) - f(x,y) \tag{6}$$

3. The proposed vessel segmentation algorithm

In the algorithm we work on the green channel f_G of the RGB color space (Fig. 2a), because blood containing features appear most contrasted in this channel.

3.1. Contrast enhancement

First, a local enhancement technique introduced in [5] is performed on the image f_G:

$$f_G^1 = LCE(f_G) \tag{7}$$

where the transformation LCE is defined in the following way:

$$LCE(x,y) = 255 \cdot \frac{\Psi_w(f) - \Psi_w(f_{\min})}{\Psi_w(f_{\max}) - \Psi_w(f_{\min})} \tag{8}$$

where sigmoidal function $\Psi_w(f)$ is defined as:

$$\Psi_w(f) = \left[1 + \exp\left(\frac{\mu_f^w - f(x,y)}{\sigma_f^w}\right)\right]^{-1} \tag{9}$$

$$\mu_f^w = \frac{1}{M} \sum_{(i,j)\in w} f(i,j) \tag{10}$$

$$\sigma_f^w = \frac{1}{M \cdot (M-1)} \sum_{(i,j)\in w} (f(i,j) - \mu_f^w)^2 \tag{11}$$

w - window of size *MxM* pixels centered on a pixel located at *(i,j)*

μ_f^w - mean intensity within w

σ_f^w - standard deviation within w

$f_{\min}$, $f_{\max}$ - minimum and maximum intensities of the whole image.

The above local contrast enhancement technique is superior to other contrast enhancement techniques for the following reasons. First, because of its 'locality' (it is not based on the global statistics of the image). Secondly, it depends on the mean and variance of the intensity within the local area. If the variation of the intensity in the local area is high, the algorithm does not increase the local contrast. On the other hand, if the intensity variation in the local area is small, the local contrast is increased. Due to these properties, the local contrast is enhanced smoothly.

Once local contrast enhancement is applied, details can be seen more clearly compared to that of the original image (see Fig. 2b).

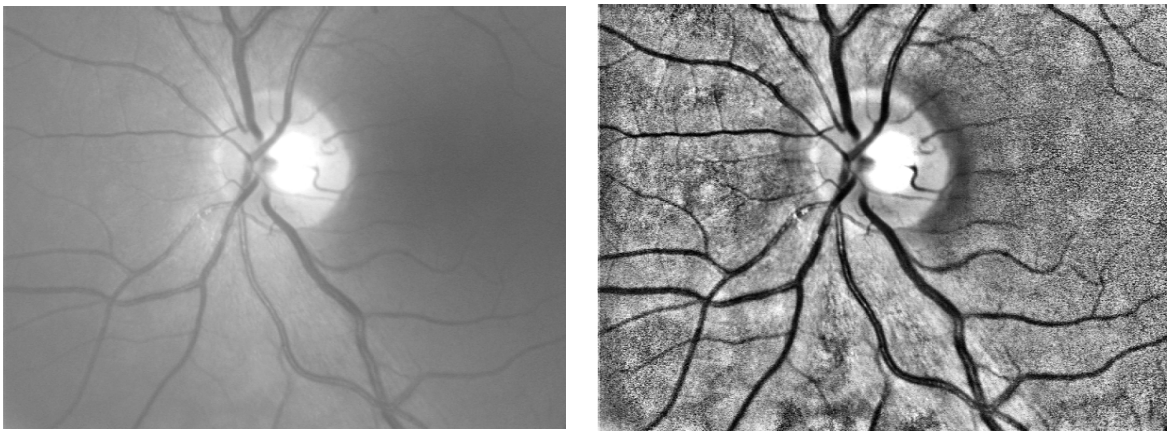

a) b)

Fig. 2. Contrast enhancement: a) channel *G* of the input image shown in Fig.1, b) channel *G* after local contrast enhancement (image f_G^1)

Rys. 2. Poprawa kontrastu: a) kanał *G* obrazu wejściowego z rys. 1, b) kanał *G* po operacji lokalnej poprawy kontrastu

3.2. Noise removing

In order to eliminate noise, we perform two-step transformation composed of a specially designed gray-level dilations followed by erosions. The first step relies on calculation the infimum of dilations with linear structuring elements B_i (*15* pixels long and *1*-pixel wide) in different directions – every 15^o.

$$f_G^2 = \inf\{D^{B_i}(f_G^1) : i = 1,...,12\} \tag{12}$$

The second step relies on calculation of the supremum of erosions with linear structuring elements B_i (*15* pixels long and *1*-pixel wide) in different directions – every 15^o:

$$f_G^3 = \sup\{E^{B_i}(f_G^2) : i = 1,...,12\} \tag{13}$$

The results of de-noising operation is shown in Fig.3a and 3b.

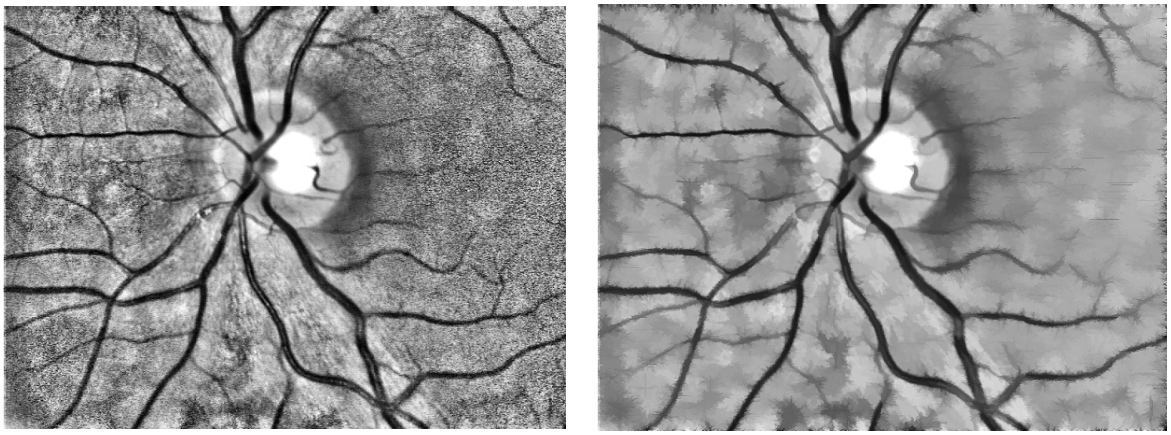

a) b)

Fig. 3. Denoising: a) image f_G^1 after applying infimum of dilations with linear structuring elements (image f_G^2), b) image f_G^2 after applying supremum of erosions (image f_G^3)

Rys. 3. Odszumianie: a) obraz f_G^1 po zastosowaniu infimum dylatacji z liniowymi elementami strukturalnymi (obraz f_G^2), b) obraz f_G^2 po zastosowaniu supremum erozji (obraz f_G^3)

3.3. Detection based on Top-Hat transformation

For the extraction of the vascular tree, on the prefiltered image from the previous step, we use *Top-Hat closing* transformation which is usually used to extract contrasted components with respect to the background:

$$f_G^4 = TH_c^B(f_G^3) \tag{14}$$

with a structuring element *B* being a circle of a radius *r*, followed by a global binarization:

$$f_G^5 = T_{T1}(f_G^4) \tag{15}$$

We use two pairs of values for a radius r of a structuring element B in *Top-Hat* transformation and a threshold *T1*:

- *r=4* and *T1=20* for thinner vessels lower contrasted (images f_G^4 and f_G^5),
- *r=11* and *T1=40* for thicker vessels better contrasted . (images $f_G^{4'}$ and $f_G^{5'}$).

Then, the two f_G^4, f_G^5 images are added:

$$f_G^6 = f_G^5 \cup f_G^{5'} \tag{16}$$

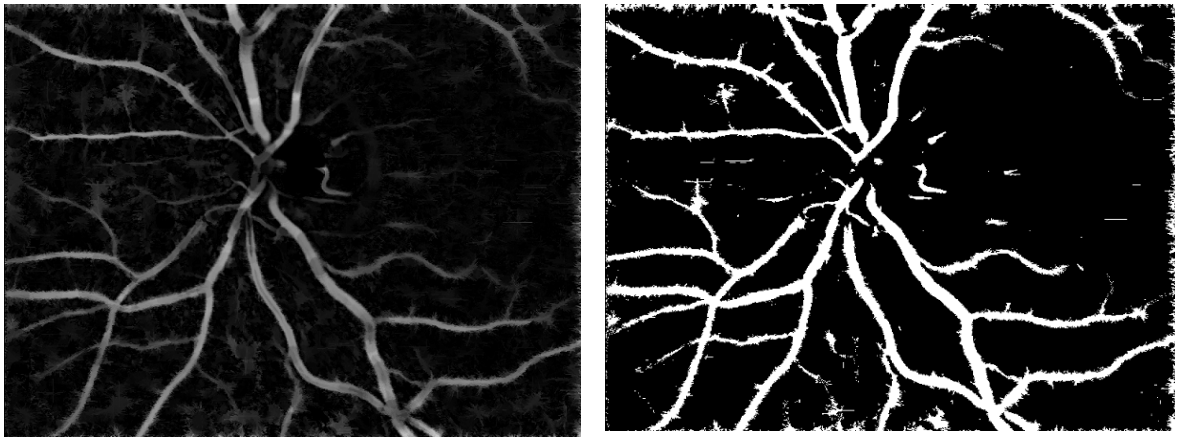

a) b)

Fig. 4. Detection: a) image f_G^3 after top-hat closing transformation, b) binarization of image shown in 4a) with *r=11*, *T1=40*

Rys. 4. Detekcja: a) obraz f_G^3 po zastosowaniu transformacji czubek-kapelusza, b) binaryzacja obrazu z rys. 4a) z *r=11* i *T1=40*

3.4. Classification

As the image f_G^6 contains some false vessels resulting from noise and poor contrast, we perform classification of the resulted regions based on their whole area and the shape coefficient describing their ‘linearity’ being the ratio of the area to perimeter. The final segmentation result is shown in Fig.5.

4. Results and conclusions

We tested the algorithm on the 50-ty color images. The results are satisfactory on most of the images (46). Smaller vessels, if not connected to the rest of the vascular tree are often missed, which is not a drawback if vessels detection is used for the image registration. There

are very few false positives (4%). However, if there are a lot of hemorrhages and microaneurysms, particularly if they are close to the vascular tree, another prefiltering step must be performed (for example infimum of closings with linear structuring elements of different directions, followed by a closing by reconstruction).

The proposed, new algorithm shall be used as a first step in image registration, for the identification of false positives in pathology detection and for the classification of the pathologies.

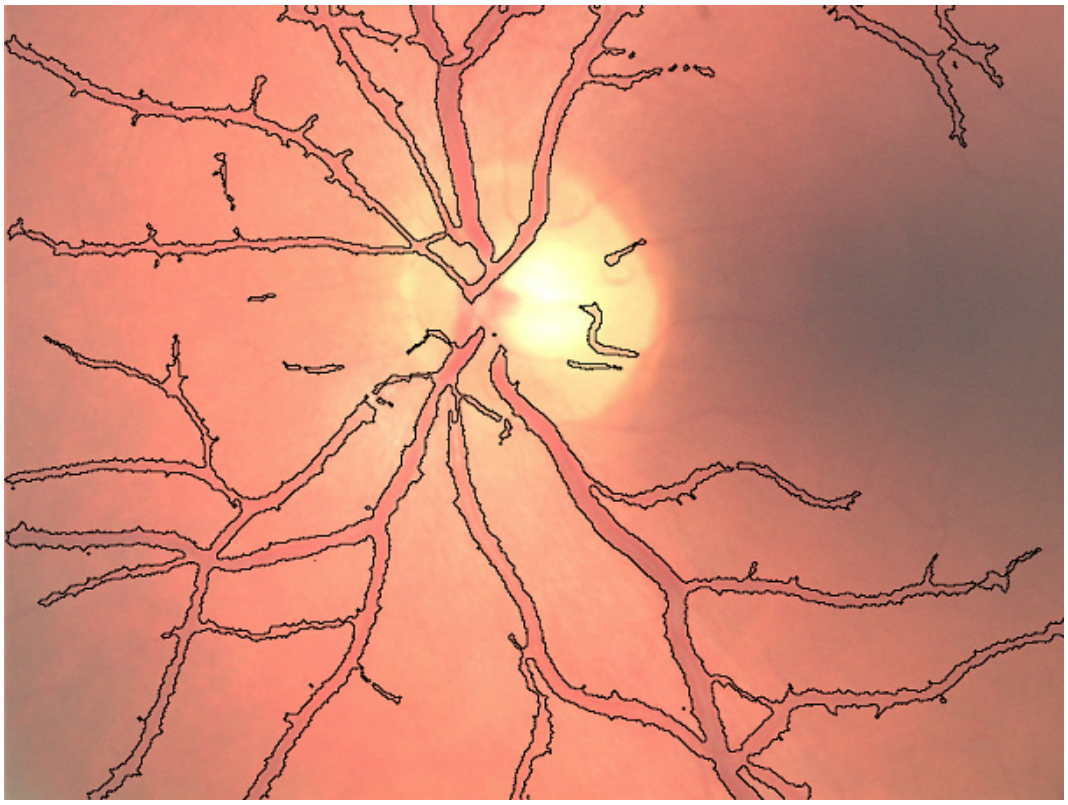

Fig. 5. The exampled fundus eye image with the detected vessels
Rys. 5. Obraz dna oka z wykrytymi naczyniami krwionośnymi

REFERENCES

1. Chaudhuri S. et al: Detection of blood vessels in retinal images using two-dimensional matched filters. IEEE Trans. Medical Imaging, v. 8, Nr 3, 1989, 263-269.
2. Gonzalez R.C, Woods R.E: Digital Image Processing. Prentice-Hall, 2002.
3. Kanski J. et al.: Clinical ophthalmology. Butterworth-Heinemann, 1996.
4. Pinz A. et al: Mapping the human retina. IEEE Trans. Medical Imaging, v. 17, Nr 4, 1998, 606-619.

5. Sinthanayothin C. et al: Automated localisation of the optic disc, fovea and retinal blood vessels from digital color fundus images. British Journal of Ophthalmology, v. 83, Nr 8, 1999, 902-910.
6. Soille P.: Morphological Image analysis: principles and applications. Springer-Verlag, Berlin 1999.
7. Tamura S. et al: Zero-crossing interval correction in tracing eye-fundus blood vessels. Pattern Recognition, v. 21, Nr 3, 1988, 227-233.
8. Zana F., Klein J. C.: Segmentation of vessel like patterns using mathematical morphology and curvature evaluation. IEEE Trans. Medical Imaging, v.10, Nr 7, 2001, 1010-1019.

Recenzent: Dr inż. Henryk Palus

Wpłynęło do Redakcji 31 marca 2004 r.

Omówienie

W artykule zaproponowano nowa metodę automatycznej segmentacji naczyń krwionośnych na cyfrowych obrazach dna oka. Metoda wykorzystuje narzędzia wieloodcieniowej morfologii matematycznej [6]. Składa się ona z następujących etapów: 1) lokalna poprawa kontrastu, 2) odszumianie, 3) detekcja naczyń, 4) klasyfikacja. W celu odszumienia zastosowano operacje złożone ze specjalnie zaprojektowanych operacji dylatacji i erozji wieloodcieniowej. Sama detekcja naczyń wykorzystuje operację czubek-kapelusza. Ostatni krok klasyfikacji wprowadzono w celu eliminacji fałszywych elementów. Rysunek 5 pokazuje rezultat opisanej metody dla przykładowego obrazu dna oka.

Adresses

Katarzyna STĄPOR: Politechnika Śląska, Instytut Informatyki, ul. Akademicka 16, 44-100 Gliwice, Polska, delta@ivp.iinf.polsl.gliwice.pl .
Adam ŚWITOŃSKI, Politechnika Śląska, Instytut Informatyki, ul. Akademicka 16, 44-100 Gliwice, Polska.